IEICE TRANS. COMMUN., VOL.E91–B, NO.3 MARCH 2008

PAPER

Two-Dimensional Target Location Estimation Technique Using Leaky Coaxial Cables

Kenji INOMATA[†a)], ***Member***, **Takashi HIRAI**[†], ***Nonmember***, **Yoshio YAMAGUCHI**[††], ***Fellow***, ***and*** **Hiroyoshi YAMADA**[††], ***Member***

SUMMARY This paper presents a target location estimation method that can use a pair of leaky coaxial cables to determine the 2D coordinates of the target. Since convention location techniques using leaky coaxial cables can find a target location along the cable in 1D, they have been unable to locate it in 2D planes. The proposed method enables us to estimate target on a 2D plane using; 1) a beam-forming technique and 2) a reconstruction technique based on Hough transform. Leaky coaxial cables are equipped with numerous slots at regular interval, which can be utilized as antenna arrays that acts both as transmitters and receivers. By completely exploiting this specific characteristic of leaky coaxial cables, we carried out an antenna array analysis that performs in a beam-forming fashion. Simulation and experimental results support the effectiveness of the proposed target location method.

key words: *position detection, leaky coaxial cable, slot array, Hough transform*

1. Introduction

Leaky coaxial cables [1]–[5] are used for wireless communication in tunnels, highway information broadcasting, train communication [6], [7], and target detection sensors [8]–[13]. In the application of target detection, a pair of leaky coaxial cables is placed along the perimeter of a surveillance area.

One cable transmits microwaves and another cable receives the waves scattered by the target as shown in Fig. 1. The target detection is performed as follows:

1) Scattered waves from a target are identified by subtraction of the previous signals in time series.
2) The propagation delay time of the scattered wave is utilized to determine the location, i.e., the distance from the source point along the cable. The distance is obtained by modulated signals such as pulse, chirp, or coded signal.

It is known from the observations that:

3) Since the target distance is measured by propagation delay time, the sensor cannot determine the target location by the distance information alone whether it is from a point along the cables or across the cables.

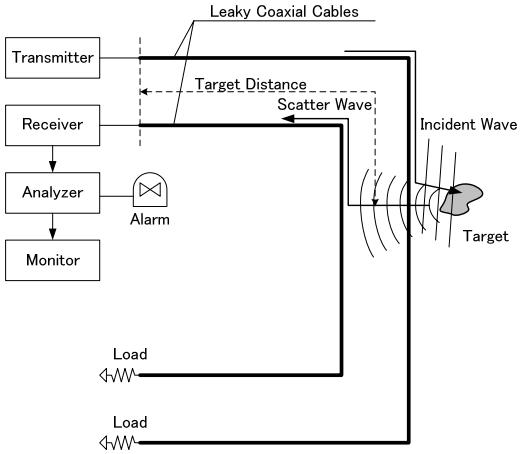

Fig. 1 Basic configuration of the system and intrusion detection applications for leaky coaxial cables.

4) If two targets are measured as having identical power and identical propagation delay time, the sensor regards them as the same target.

The purpose of this paper is to establish a 2-dimensional (2D) target location estimation technique using leaky coaxial cables and to experimentally show its availability. In this target location estimation, a beam-forming technique using leaky coaxial cables is the most important factor for 2D surveillance. The directivity of leaky coaxial cables and the frequency bandwidth have been studied under several geometrical conditions assuming an infinite length of leaky coaxial cable having infinite number of slots [1]–[3]. However, in the experiment, we have to treat a finite length of leaky coaxial cable having finite number of slots. Therefore we applied an array antenna analysis to find the directivity of finite number of slots in leaky coaxial cable. The relation between the directivity and the operation frequency of short leaky coaxial cable (50 m) are presented by numerical simulation. Since the radiation angle changes by frequency, the response property of scattered signal, e.g. propagation delay time, changes according to frequency.

We propose a target location estimation technique using this frequency-dependent time delay property. This technique determines a 2D target location from the responses of multiple frequencies by Hough transform. We carried out a 2D imaging experiment to confirm the theory.

In this paper, we formulate the directivity of infinite

Manuscript received March 26, 2007.
Manuscript revised August 10, 2007.
[†]The authors are with Mitsubishi Electric Corp., Amagasaki-shi, 661-8661 Japan.
[††]The authors are with Niigata University, Niigata-shi, 950-2181 Japan.
a) E-mail: inomata.kenji@dy.MitsubishiElectric.co.jp
DOI: 10.1093/ietcom/e91–b.3.878

leaky coaxial cables and the target response by leaky coaxial cables for transmitter and receiver in Sect. 2, and a 2D target reconstruction method in Sect. 3. Section 4 provides numerical verification of the method by comparing the properties of leaky coaxial cables of finite and infinite lengths. In Sect. 5, the results of field experiments are presented and discussed.

2. Target Response by Leaky Coaxial Cables and Problem Formulation

2.1 Configuration of Leaky Coaxial Cables

Leaky coaxial cables transmit and receive microwaves by slots milled in outer conductors at regular intervals P [1]–[5]. While many milling slot patterns have been proposed, the currently available leaky coaxial cables can be categorized into two types: surface wave and radiating wave. In this paper we use the latter type.

The slot interval of basic leaky coaxial cables is associated with wavelength, as shown in Fig. 2(a). On the inclined slot at angle ϕ, magnetic current J_m appears by the difference of magnetic potential on the slot. Since the magnitude of J_m is dependent on the angle ϕ, ϕ is a factor related to the antenna gain and the resultant coupling loss.

Since the effective bandwidth of basic leaky coaxial cables is narrow, several configurations have been proposed to expand the bandwidth by inserting subslots [1], [2], [5], [6]. We used 1/6, 1/2, and 2/3 subslots as shown in Fig. 2(b).

2.2 Directivity of Leaky Coaxial Cable

Consider the N slot array shown in Fig. 3. We assume that narrow-band signal s arrives at the array from angle θ, and that the source is located in the far field. Slot array output E_r is then

$$E_r = \boldsymbol{v}^T \boldsymbol{a}(\theta) s + \boldsymbol{v}^T \boldsymbol{n}(t), \tag{1}$$

where $\boldsymbol{a}(\theta)$ denotes the mode vector to a plane wave of unit amplitude arriving from direction θ, $n(t)$ is a vector of additive noise that represents the effect of the undesired signal, and $(\cdot)^T$ denotes the transpose. $\boldsymbol{v}$ is a weight vector defined by

$$\boldsymbol{v} = [L_1 \exp(-jk'd_1) \ldots L_N \exp(-jk'd_N)]^T, \tag{2}$$

where L_n is the nth coupling loss factor between elements and subsequent amplification, k' is the wave number in the leaky coaxial cable, and d_n is the distance from the reference point depicted in Fig. 3 to the nth slot.

Now, $|L_n| = L_0$. Under the configuration of leaky coaxial cable describing in Fig. 3, vector $\boldsymbol{L}$ is then

$$\boldsymbol{L} = [L_0\ L_0\ -L_0\ -L_0\ L_0 \cdots]^T, \tag{3}$$

where the sign of L_0 is positive if slot angle $\phi \geq 0$, and negative if slot angle $\phi < 0$, as depicted by black and white dots, respectively.

Thus the radiation pattern is obtained by

$$D(\theta, f) = \frac{1}{2} \left| \boldsymbol{v}^T \boldsymbol{a}(\theta) \right|^2, \tag{4}$$

where

$$\boldsymbol{a}(\theta) = \left[e^{-j\frac{2\pi f}{c} d_1 \sin\theta}\ e^{-j\frac{2\pi f}{c} d_2 \sin\theta}\ \ldots\ e^{-j\frac{2\pi f}{c} d_N \sin\theta} \right]^T, \tag{5}$$

c is wave the velocity in free space, and f is the center frequency.

2.3 Target Response by Leaky Coaxial Cables

Consider two leaky coaxial cables located in parallel, as shown in Fig. 4. The signal radiated from the transmitting leaky coaxial cable is scattered by the target. For simplicity, we assume the target is an isotropic object since the location estimator described later is not affected by receiving magnitude, under the condition that signal noise ratio (SNR) is sufficient.

Since $\boldsymbol{a}(\theta)$ denotes the mode vector of a plane wave, we replace it by propagation vector $\boldsymbol{p}$ associated with the location of both the target and each slot (9). Ignoring some coefficients, incident signal from the transmitting leaky coaxial cable to the target can be written by

$$E_i = \boldsymbol{v}^T \boldsymbol{p} E_0 = \boldsymbol{p}^T \boldsymbol{v} E_0, \tag{6}$$

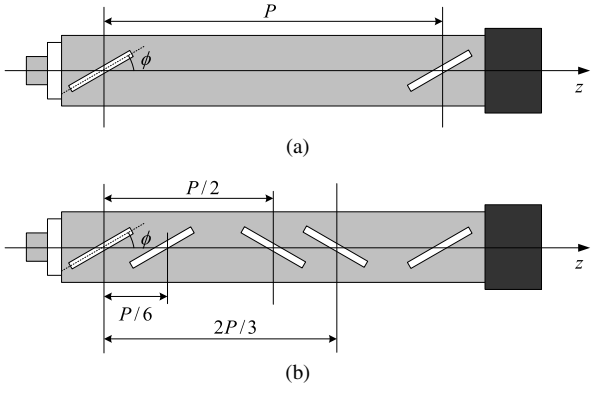

Fig. 2 Configuration of leaky coaxial cables: (a) basic configuration: (b) wide bandwidth configuration with subslot.

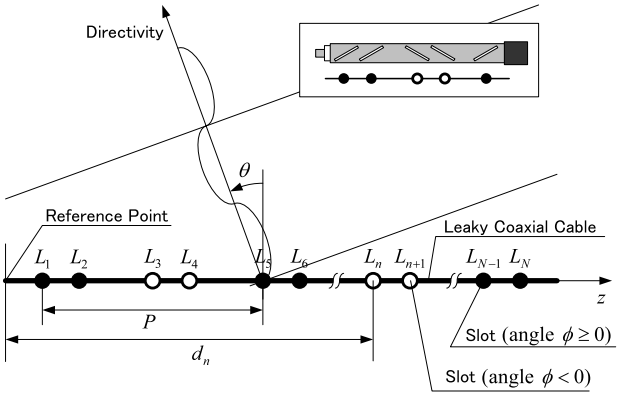

Fig. 3 Slot array model of leaky coaxial cable.

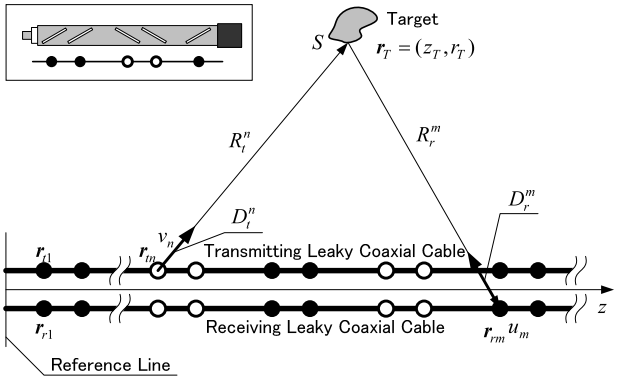

Fig. 4 Analysis model for target response.

where E_0 is an input signal to the transmitting leaky coaxial cable.

The target response by the receiving leaky coaxial cable is then

$$E_s = \boldsymbol{w}^T \boldsymbol{q} E_T, \tag{7}$$

where E_T is the scattered signal of the target, $\boldsymbol{w}$ is a weight vector of the receiving leaky coaxial cable, and $\boldsymbol{q}$ is a propagation vector associated with $\boldsymbol{p}$.

Using (6) and (7), target response E_S becomes

$$E_s = \boldsymbol{w}^T \boldsymbol{q} S \boldsymbol{p}^T \boldsymbol{v} E_0, \tag{8}$$

where S is the scattering coefficient. For simplicity, the polarization is ignored because the SNR influenced by the polarization does not affect the estimator, under the condition that the SNR is adequate.

We define $\boldsymbol{r}_T$ as a position vector of the target, $\boldsymbol{r}_t^n$ is the nth slot position vector of the transmitting leaky coaxial cable, and $\boldsymbol{r}_r^m$ is the mth slot position vector of the receiving leaky coaxial cable. Propagation vectors $\boldsymbol{p}$ and $\boldsymbol{q}$ are expressed by

$$\begin{aligned} \boldsymbol{p} &= [D_t^1 \exp(-jkR_t^1)/R_t^1 \cdots D_t^N \exp(-jkR_t^N)/R_t^N]^T, \\ \boldsymbol{q} &= [D_r^1 \exp(-jkR_r^1)/R_r^1 \cdots D_r^M \exp(-jkR_r^M)/R_r^M]^T, \end{aligned} \tag{9}$$

where k is the wave number in free space,

$$\begin{aligned} R_t^n &= \left|\boldsymbol{r}_T - \boldsymbol{r}_t^n\right| \text{ and} \\ R_r^m &= \left|\boldsymbol{r}_T - \boldsymbol{r}_r^m\right|, \end{aligned}$$

where D_t^n is the directivity at the direction of the nth slot on the transmitting cable toward the target, and D_r^m is that of the mth slot on the receiving cable.

Equation (8) holds for an arbitrary form of leaky coaxial cables. However, for problem simplicity we consider straight forms of leaky coaxial cables with regular intervals.

3. Two-Dimensional Target Location Method

One method for obtaining target response in the time domain is the Fourier transform of target frequency response. Using frequency response $E_s(f)$ of the target given by (8), the time domain response is written by

$$T_s(t) = FFT^{-1}[E_s(f)], \tag{10}$$

where $FFT^{-1}[\cdot]$ denotes the inverse fast Fourier transform. The propagation delay time of the target response can be discriminated by the peak of the time response.

Consider propagation delay time in geometrical terms. The property of radiation angle θ associated with frequency is needed. For the periodic structure of leaky coaxial cables, ignoring some coefficients, the field can be written by [1], [5],

$$E = E_p(\varsigma r) e^{-jk'z}, \tag{11}$$

where $\varsigma^2 = k^2 - k'^2$ is the wave number in the radial direction, E_p is the periodic function of z that can be expressed in Fourier series as

$$E_p(\varsigma r) = \sum_{u=-\infty}^{\infty} E_{pu}(\varsigma_u r) e^{-j\frac{2u\pi}{P}z}. \tag{12}$$

Thus

$$E = \sum_{u=-\infty}^{\infty} E_{pu}(\varsigma_u r) e^{-jk'_u z}, \tag{13}$$

where $k'_u = k' + 2u\pi/P$, $k' = \sqrt{\varepsilon_r}k$, ε_r is relative permittivity. The wave number of the uth harmonic in the radial direction is written by

$$\varsigma_u = \sqrt{k^2 - k'^2_u}. \tag{14}$$

When ς_u is real, the leaky coaxial cable acts in a radiation mode, and frequency bandwidth in the uth harmonic is

$$-uf_L \le f \le -uf_H, \tag{15}$$

where $f_L = c/P(\sqrt{\varepsilon_r} + 1)$ and $f_H = c/P(\sqrt{\varepsilon_r} - 1)$. If we use the range of $f_L < f < 2f_L$, then only the -1th harmonic occurs. However the range of $2f_L < f$ yields unwanted multiple beams. Since the unwanted beams generate multiple target responses in each target, interfering with the identification of the individual target response, we use a single radiation mode for the 2D target location estimation.

Radiation angles θ_u are determined by

$$\theta_u = \sin^{-1}(-\sqrt{\varepsilon_r} - u\lambda/P), \tag{16}$$

where $\lambda = c/f$ is the wavelength.

Here, we use the -1th angle $\theta = \theta_{-1}$. The round-trip path is depicted by arrows in Fig. 5. To derive propagation delay time easily, we assume that the interval between transmitting and receiving cables is much smaller than the spatial resolution defined by the observing bandwidth. The transmission delay time t_1 in the leaky coaxial cables and the propagation delay time t_2 in the free space are respectively defined using the target location (z_T, r_T) as follows:

$$t_1 = t_z + t_2 \sqrt{\varepsilon_r} \sin\theta, \tag{17}$$

$$t_2 = t_r / \cos\theta, \tag{18}$$

where $t_z = z_T/c'$, $t_r = r_T/c$, c' $(= c/\sqrt{\varepsilon_r})$ is the wave velocity in the cable. The propagation delay time is written as

$$T = 2(t_1 + t_2). \tag{19}$$

Using, (17), (18), we can obtain,

$$T = 2[z_T/c' + r_T(\sqrt{\varepsilon_r}\tan\theta + 1/\cos\theta)/c]. \tag{20}$$

T is a function of observation frequency f because θ is the function of f.

Assuming $\theta \ll 1$, then we obtain $\tan\theta \approx \sin\theta$ and $1/\cos\theta \approx 1$. Equation (20) can be simplified to

$$T \approx b + af^{-1}, \tag{21}$$

where

$$a = 2r_T/\kappa P \text{ and}$$
$$b = 2(z_T/\kappa + r_T - r_T/\kappa^2)/c,$$

where $\kappa = 1/\sqrt{\varepsilon_r}$ is the contraction rate in the leaky coaxial cable.

Target location $\boldsymbol{r}_T = (z_T, r_T)$ can be obtained by solving the simultaneous equation of (21) using two frequencies, if the number of targets is one. We propose a target reconstruction technique for multiple targets in three steps:

1) We measure target response with multiple frequencies to create a frequency versus time response plane (*f-t* plane);
2) We project the *f-t* plane to a parameter field associated with $T = b + af^{-1}$ using Hough transform;
3) To estimate the target location, we transform the parameter field to the target's coordinate field and detect the peak points in it.

The Hough transform yields the parameters of lines or circles in a binary image [14], [15]. A point in the *f-t* plane is projected to the parameter field as a curved line. After projecting from all points of the *f-t* plane, the parameter of the curved line is obtained by searching for the peak point in the parameter field. Since there is no noise, the number of peaks equals the number of the curves. However, since the Hough transform is usually used for finding straight lines, we apply it to obtain the parameter field of a function $T(f) = b + af^{-1}$.

Using (21), the transform equation from the parameter field to the target's coordinate field is expressed as

$$\begin{pmatrix} z_T \\ r_T \end{pmatrix} = \begin{pmatrix} (\kappa P/2)(1/\kappa - \kappa) & \kappa c/2 \\ \kappa P/2 & 0 \end{pmatrix} \begin{pmatrix} a \\ b \end{pmatrix}. \tag{22}$$

This target reconstruction technique assumes an infinite length of leaky coaxial cable, because (16) assumes an infinite leaky coaxial cable. However, in general case, cable length is not infinite. Sometimes short leaky coaxial cables are needed. Therefore, verifying the effects of finite length of the leaky coaxial cable is important.

4. Numerical Example

4.1 Directivity of Leaky Coaxial Cables

We verify the directivity of (4) for the finite length depicted in Fig. 2(b) compared to that of (16) for infinite length. Using (4), the specification of leaky coaxial cables is shown in Table 1. The directivity of finite length is depicted as gray lines in Fig. 6, whereas that of infinite length is indicated as dashed lines.

As shown in Fig. 6, the finite length of the leaky coaxial cable yields the same pattern as an infinite cable at $u = -1$. The radiation modes of $u = -2$, -3, -4, and -6 are eliminated due to the effect of the subslots. A half pitch subslot eliminates the $2u$ mode beam, and a 1/6 pitch subslot eliminates the $3u$ mode beam. This subslot expands the single mode bandwidth. Therefore the advantage of using (4) at u

Table 1 Leaky coaxial cable specifications for numerical simulations.

1. Length	50 m
2. Contraction rate	0.867
3. Attenuation	0.03 dB/m
4. Main slot pitch	1.032m
5. Subslot pitch	1/2, 2/3 (inverse phase), 1/6 (in-phase)

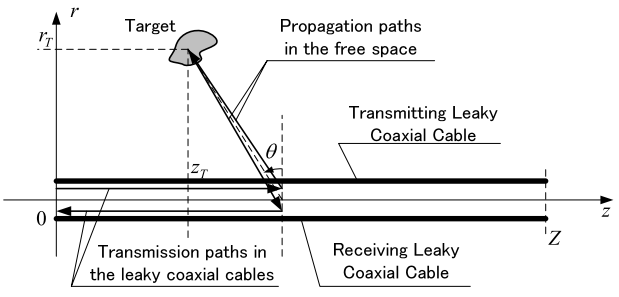

Fig. 5 Analysis model.

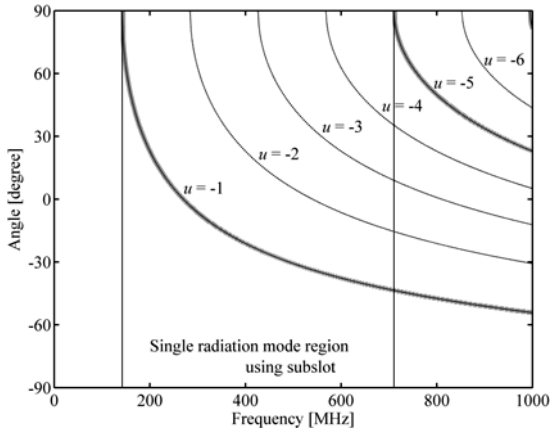

Fig. 6 Computation results of directivity of leaky coaxial cables.

$= -1$ can be recognized.

4.2 Target Response by Leaky Coaxial Cable

We simulated target responses to verify the former's availability comparing (20) with (10). We assume that the target is an isotropic scattering object smaller than the spatial resolution and the target reflection coefficient is 1.

A leaky coaxial cable, whose specifications are shown in Table 1, is set parallel at 1 m intervals. Target locations are $(z_T, r_T) = (20, 1)$ and $(20, 5)$ [m], respectively.

To obtain multi-frequency target responses, we compute the responses using (8) whose center frequency ranges from 250 to 400 MHz. The radiation angle changes from 5.2 to -21.2 degrees respectively. To calculate the propagation delay time to generate *f-t* plane, (10) is carried out with 60 MHz bandwidth.

The simulation results of the *f-t* plane are shown in Fig. 7. The horizontal axis is the frequency range, and the vertical axis is the propagation delay time. Normalized power density is depicted in grayscale. In Fig. 7(a), the target is close to the leaky coaxial cable, and the difference of propagation delay time is small at each radiation angle. Hence the time response is nearly flat all over the entire frequency range. In Fig. 7(b), since the target is distant from the leaky coaxial cables, it is illuminated at various radiation angles. Hence the time response varies with frequency.

Theoretical delay time using (20) is indicated in a dashed line on the grayscale density image. These results demonstrate the availability of using (20) as an infinite cable. Since we usually assume that cable length is longer than this case, (20) is available in most situations.

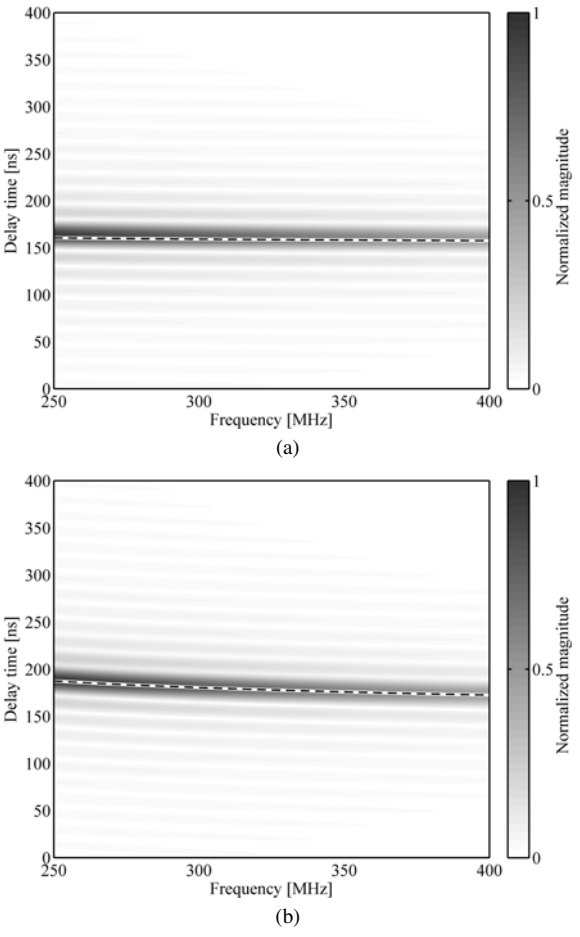

Fig. 7 Simulation results of observation frequency versus delay time of targets: (a) $(z_T, r_T) = (20, 1)$, (b) $= (20, 5)$ [m].

5. Experimental Results of Two-Dimensional Target Location Estimation Using Leaky Coaxial Cables

5.1 Configuration of Experimental Test Circuits

A simplified multi-frequency microwave transceiver, shown in Fig. 8, is connected to the leaky coaxial cables using approach cables. Transmitting frequency of the oscillator (OSC) is controlled by the Digital Signal Processor. Generated continuous wave is radiated from the transmitting leaky coaxial cable, and direct and reflected waves are received by the receiving leaky coaxial cable. Terminators are connected at the end of the leaky coaxial cables to absorb the co-coupling signals. To obtain the scattered signal from the target, the received signal is subtracted from the initial value previously measured.

The specifications of the leaky coaxial cable are shown in Table 1. They are arranged on dry ground, as shown in Fig. 9, in nearly identical configuration as in Fig. 5.

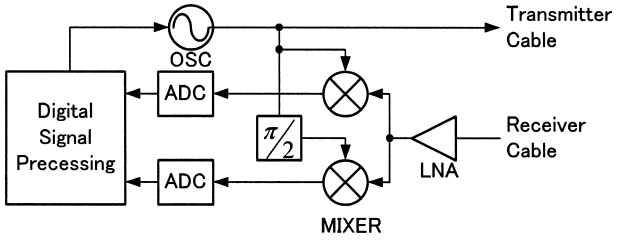

Fig. 8 Construction of field test circuits.

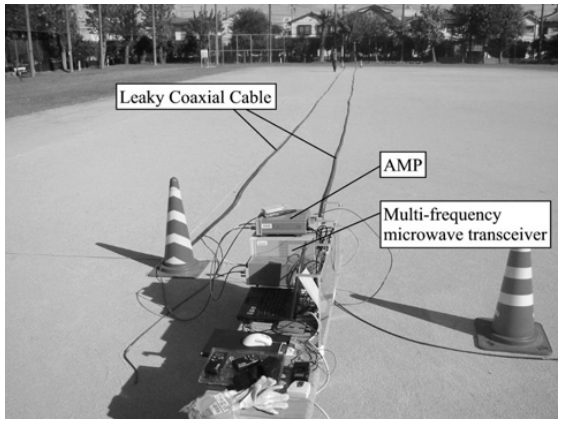

Fig. 9 Validation system of two-dimensional target location by leaky coaxial cables.

Fig. 10 Experiment target.

The measuring frequency band ranges 220 to 430 MHz at 0.25 MHz intervals. The analysis bandwidth for the Fourier transform is 60 MHz. Therefore, the frequency band of the *f-t* plane is from 250 to 400 MHz.

We used a vehicle ($1.96 \times 1.69 \times 4.68$ m) as a target shown in Fig. 10. Since this target size nearly equals spatial resolution, we decide to use the vehicle because this big target generates large scattering signals easily.

5.2 Experimental Results of Target Response

We experimented with two target locations. One is location estimation when it is changed to the leaky coaxial cable direction, and the other is when the target location is changed to a vertical direction of the leaky coaxial cables. In the first experiment, target positions were (z_T, r_T) = (10, 1), (30, 1), (50, 1) [m]. The origin is the middle of two leaky coaxial cable tips, which are the sides connecting the transceiver with approach cables. The target's origin is the center of the vehicle's front bumper.

The experimental results of the *f-t* plane are depicted in Fig. 11 as normalized power density. The dashed line in Fig. 11 is the theoretical result using (20).

These results show that the theoretical lines approximately agree with the experimental results. However, two or three peaks appear at some frequency range in the *f-t* plane, because the target's radar cross section is not constantly associated with the incident wave angle determined by the frequency. The uncertainty of this response probably influences target location estimation accuracy.

Figures 12(a), (b), and (c) show the target reconstruction images by Hough transform associated with Fig. 11. To show the peak clearly, we emphasize the grayscale level grater than that of 0.95 in Fig. 12. The peak points of Figs. 12(a), (b), and (c) are (z_T, r_T) = (11.0, 1.5), (28.5, 1.0), and (48.5, 1.5), respectively, whereas the points of the target were (z_T, r_T) = (10, 1), (30, 1), (50, 1). The maximum error in these experiments was 1.5 m. This accuracy is sufficient for the application since the error was smaller than the spatial resolution. The spatial resolution is 2.5 m, which is determined by observation band width of 60 MHz. Furthermore, since two or three peaks appear in the *f-t* plane, the number of peaks in the reconstruction image is one. Thus the reconstruction method accurately estimates the number of targets.

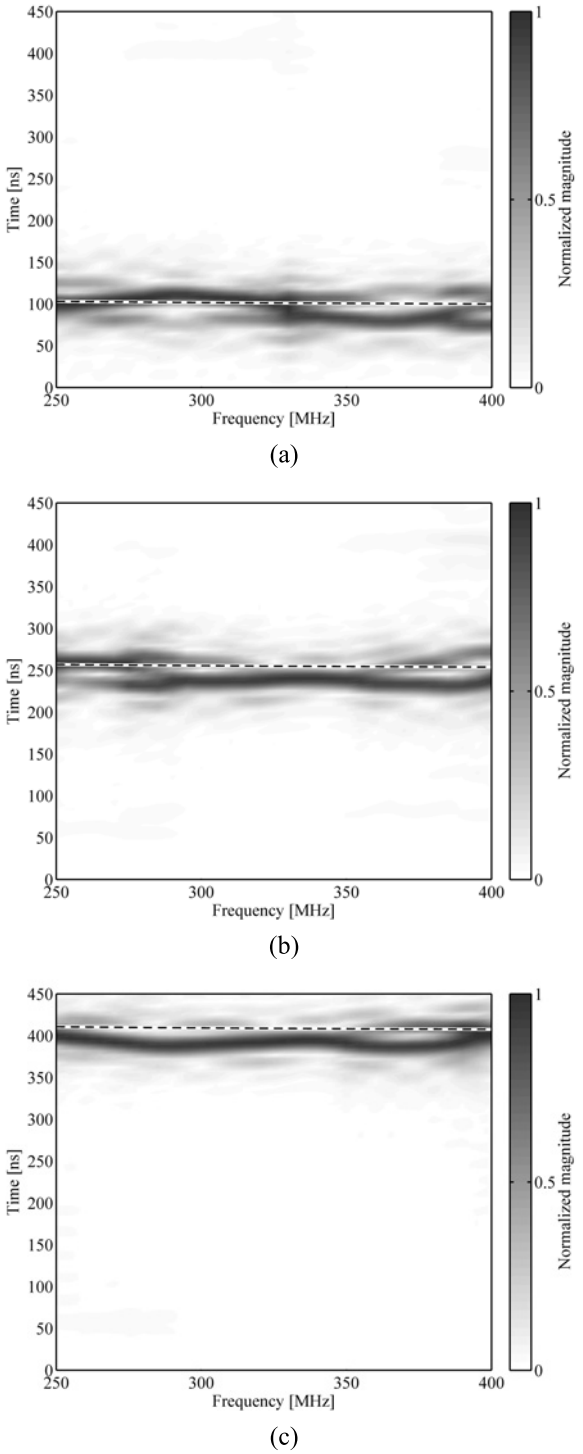

Fig. 11 Experimental results of delay time distribution with respect to frequency of the target: (a) (z_T, r_T) = (10, 1), (b) = (30, 1), and (c) = (50, 1) [m]; dashed line is theoretical delay time.

We define the increment rate of the propagation delay

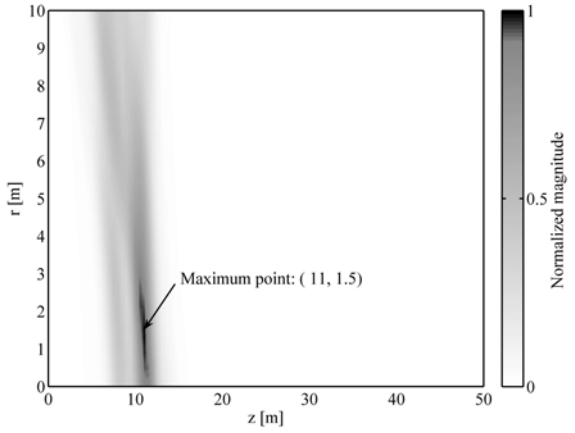

(a)

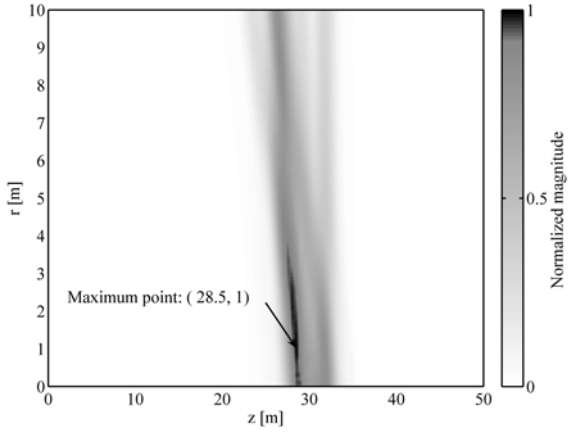

(b)

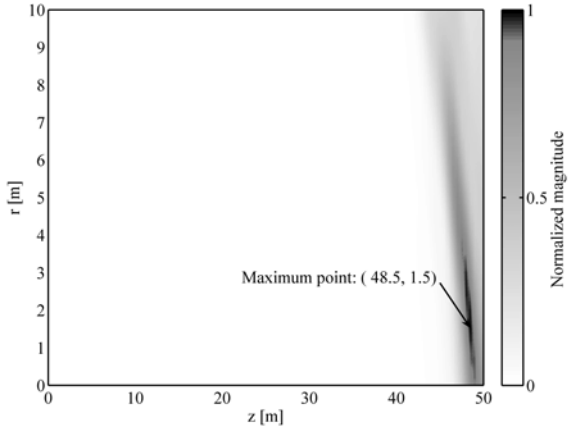

(c)

Fig. 12 Reconstruction image based on Hough transform of target: (a) $(z_T, r_T) = (10, 1)$, (b) = (30, 1), and (c) = (50, 1) [m].

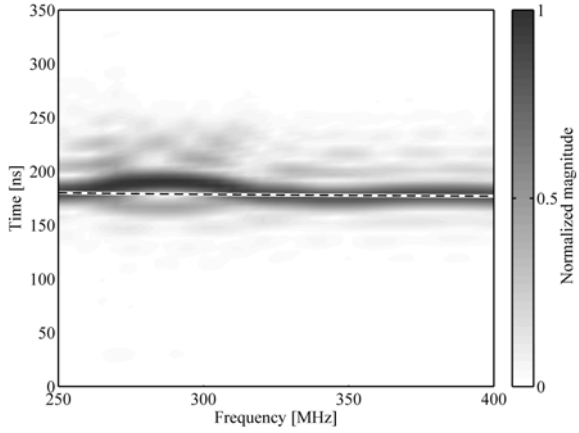

(a)

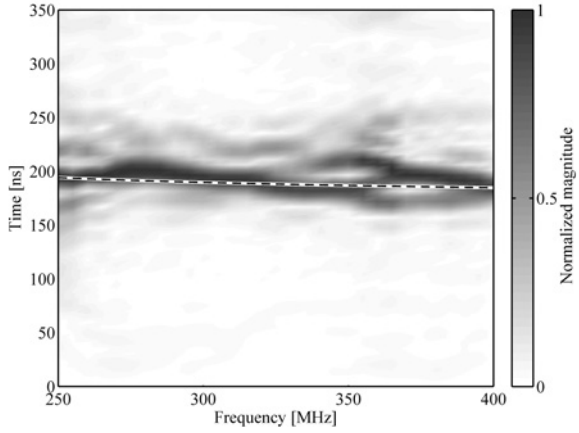

(b)

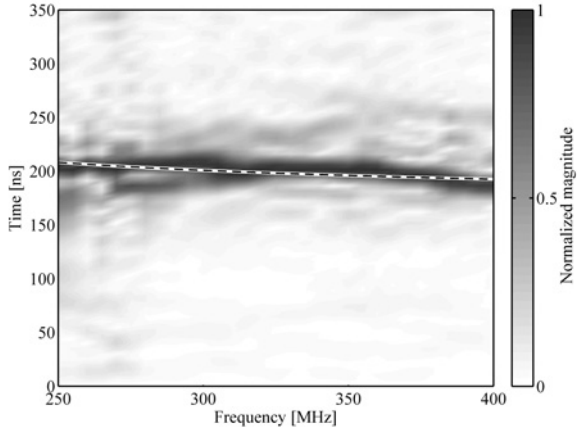

(c)

Fig. 13 Experimental results of delay time distribution with respect to frequency of the target: (a) $(z_T, r_T) = (20, 1)$, (b) = (20, 3), and (c) = (20, 5) [m]; dashed line is theoretical delay time.

time:

$$\delta = \frac{\Delta T}{\Delta z_T}, \tag{23}$$

where ΔT is increment rate of delay time of scattered signal, Δz_T is the distance to the target. The increment rate δ can be calculated using the least square method from the results depicted in Fig. 12. As a result of calculation, it is found to be $\delta = 3.7286$ nsec/m. While contraction rate κ is described as $\kappa = 1/c\delta$, the contraction rate is determined to be 0.894. This result is close to the specifications in Table 1. Furthermore, 0 m offset became 19.25 ns, which corresponds to the

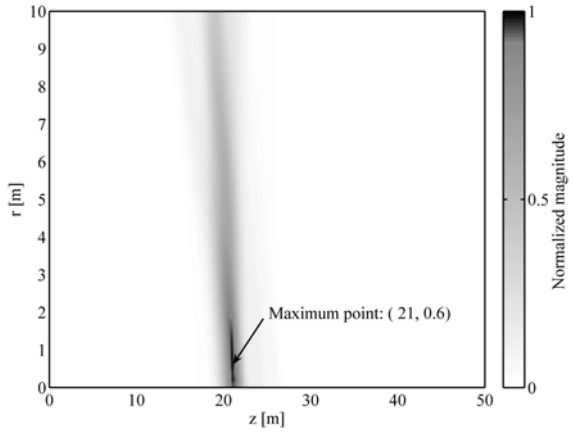

(a)

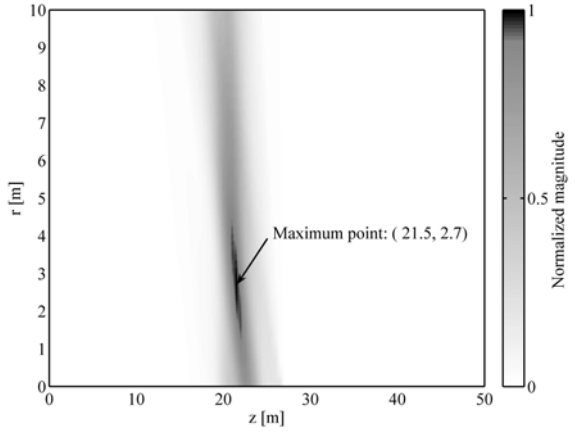

(b)

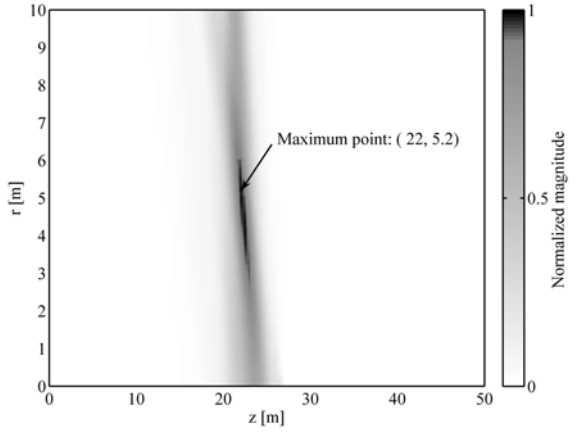

(c)

Fig. 14 Reconstruction image based on Hough transform of target: (a) (z_T, r_T) = (20, 1), (b) = (20, 3), and (c) = (20, 5) [m].

propagation delay time in the approach cable. The effect of this offset has been included in these theoretical lines.

In the second experiment, we measured targets whose positions are (z_T, r_T) = (20, 1), (20, 3), and (20, 5). The experimental results of the *f*-*t* plane are shown in Fig. 13. Theoretical delay time using (14) with offset time is indicated on the density image as a dashed line. These results show that the theoretical lines approximately agree with experimental results. Using these measured results, the target reconstruction images associated with Fig. 13 are calculated as shown in Fig. 14 respectively. We emphasize the grayscale level as in Fig. 12. The peak points of Figs. 14(a), (b), and (c) are (z_T, r_T) = (21.0, 0.6), (21.5, 2.7), and (22.0, 5.2), respectively. Target location is estimated within an accuracy of 2.5 m. In addition, the number of peaks in the reconstruction image is one in this case too. These experimental results demonstrate that our proposed target reconstruction technique based on Hough transform can estimate a target's two-dimensional location with high accuracy.

6. Conclusion

We used a pair of leaky coaxial cables as array antenna system and discussed the time-domain response of the target. We proposed a two-dimensional target location estimation technique based on Hough transform. Target location can be estimated from the multiple-frequency response of the target, which is used for finding the curved line parameters that can transform target location parameters using Hough transform.

The proposed method was verified with both numerical simulations and experiment. The results of a two-dimensional target location estimation technique showed that the locations were estimated within 2 m accuracy under 250–400 MHz bandwidth measurements.

References

[1] T. Sintani, M. Hori, and Y. Yamaguchi, "Wide-band leaky coaxial cable," Dainitch-Nihondensen-Jihou, vol.47, March 1971.
[2] T. Sindo and M. Hori, "Electric characteristics of leaky coaxial cable," Dainitch-Nihondensen-Jihou, vol.60, Sept. 1975.
[3] P.P. Delogne and A.A. Laloux, "Theory of the slotted coaxial cable," IEEE Trans. Microw. Theory Tech., vol.MTT-28, no.10, pp.1102–1107, Oct. 1980.
[4] S.T. Kim, G.H. Yun, and H.K. Park, "Numerical analysis of the propagation characteristics of multiangle multislot coaxial cable using moment method," IEEE Trans. Microw. Theory Tech., vol.46, no.3, pp.269–279, March 1998.
[5] J.H. Wang and K.K. Mei, "Theory and analysis of leaky coaxial cable with periodic slots," IEEE Trans. Antennas Propag., vol.49, no.12, pp.1723–1732, Dec. 2001.
[6] K. Matsumoto, Y. Yokoyama, M. Hanafusa, and T. Nakamura, "A new train radio-telephone system for the Tokaido Shinkansen," Mitsubishi Denki Giho, vol.63, pp.64–69, 1989.
[7] K. Matsumoto, Y. Yokoyama, S. Matsumoto, S. Arimura, and S. Fujita, "A new communication network for the Tokaido Sinkansen," Mitsubishi Denki Giho, vol.64, pp.11–17, 1990.
[8] N.A.M. Mackay and J.C. Beal, "Guided radar for obstacle detection in ground transportation system," IEEE Antennas and Prop. Society International Symp., vol.16, pp.302–305, May 1978.
[9] M.C. Maki and W. Feller, "A new air-mounted perimeter security technology," Carnahan Conf. (ICCST1988), pp.31–33, Oct. 1988.
[10] K. Harman and B. Hodgins, "Next generation of guidar technology," IEEE A&E System Magazine, vol.20, no.5, pp.16–26, May 2005.
[11] K. Inomata and T. Hirai, "Microwave back-projection radar for wide-area surveillance system," European Radar Conf. 2004, pp.89–92, 2004.

[12] K. Inomata, T. Hirai, K. Sumi, and K. Tanaka, "Wide-area surveillance sensor with leaky coaxial cables," SICE-ICASE International Joint Conf. 2006, pp.959–963, Oct. 2006.
[13] K. Inomata, T. Hirai, H. Yamada, and Y. Yamaguchi, "2-dimensional measuring method using a wide-area surveillance sensor with leaky coaxial cables," EuMA2006 Radar Conf., pp.202–205, Sept. 2006.
[14] N. Aggarwal and W.C. Karl, "Line detection in images through regularized Hough transform," IEEE Trans. Image Process., vol.15, no.3, pp.582–591, March 2006.
[15] F. O'Gorman and M.B. Clowes, "Finding picture edges through collinearity of feature points," IEEE Trans. Comput., vol.C-25, no.4, pp.449–456, April 1976.

Kenji Inomata received a B.S. degree in information engineering from Niigata University, Niigata, Japan in 1994 and a M.S. degree in information engineering from the Niigata University Graduate School of Science and Technology in 1996. He is currently with the Mitsubishi Electric Corporation, Advanced Technology R&D Center, Japan. His research interests include radar sensing technology, radar SAR, and radar polarimetry. He is a member of IEEE.

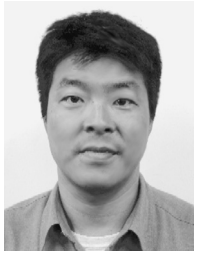

Takashi Hirai received B.S., M.S., and Ph.D. degrees from Kyoto University in 1984, 1986, and 1989 respectively. He is currently with the Mitsubishi Electric Corporation, Advanced Technology R&D Center, Japan. His research interests include security system, equipment inspection system and wireless sensors.

Yoshio Yamaguchi received a B.E. degree in electronics engineering from Niigata University in 1976 and M.E. and Ph.D. degrees in engineering from the Tokyo Institute of Technology in 1978 and 1983, respectively. In 1978, he joined the Faculty of Engineering, Niigata University, where he is a professor. During 1988 and 1989, he was a research associate at the University of Illinois, Chicago. His interests include the propagation characteristics of electromagnetic waves in a lossy medium, radar polarimetry, and microwave remote sensing and imaging. He is a fellow of IEEE.

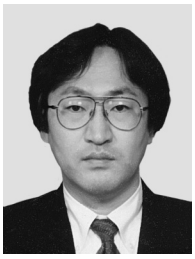

Hiroyoshi Yamada received the B.E., M.E. and Ph.D. degrees in electronic engineering from Hokkaido University, Sapporo, Japan, in 1988, 1990 and 1993, respectively. In 1993, he joined the Faculty of Engineering, Niigata University, where he is an associate professor. From 2000 to 2001, he was a Visiting Scientist at the Jet Propulsion Laboratory, California Institute of Technology, Pasadena. His current interests include superresolution techniques, array signal processing, and microwave remote sensing and imaging. He is a member of IEEE.